Clinical & Experimental IMMUNOLOGY

OXFORD

Research Article

The effects of maternal anti-alpha-enolase antibody expression on the brain development in offspring

Wei Sun[1,‡], Yan Feng[1,2,‡], Hui Li[1], Xiaoqing He[1], Yihan Lu[1,3], Zhongyan Shan[1], Weiping Teng[1], and Jing Li[1,*]

[1]Department of Endocrinology and Metabolism, Institute of Endocrinology, NHC Key Laboratory of Diagnosis and Treatment of Thyroid Diseases, The First Hospital of China Medical University, Shenyang 110001, PR China
[2]Present address: Department of Gastroenterology, The First Affiliated Hospital of Chengdu Medical College, Chengdu 610000, PR China
[3]Present address: Department of International Clinic, The Second Hospital of Dalian Medical University, Dalian 116000, PR China
‡These authors contributed equally to this work and share the first authorship.
*Correspondence: Jing Li, Department of Endocrinology and Metabolism, Institute of Endocrinology, NHC Key Laboratory of Diagnosis and Treatment of Thyroid Diseases, The First Hospital of China Medical University, 155 Nanjing North Street, Shenyang 110001, PR China. Email: lijingendocrine@126.com; jli23@cmu.edu.cn

Abstract

Anti-alpha-enolase autoantibodies have not only been found to play an important role in autoimmune diseases but also cause neurological damage in adults. In this study, a pregnant mouse model with high serum alpha-enolase (ENO1)-specific antibody (ENO1Ab) was established by immunization with ENO1 protein to explore the effects of maternal circulatory ENO1Ab on the brain development in offspring. The pups showed impaired learning and memory abilities with obviously thinner tight junctions in the brain tissue. IgG deposits colocalized with both ENO1 protein and complement 3 (C3), and the membrane attack complex was obviously detectable in the brain tissues of pups from dams with high serum ENO1Ab expression. Our findings suggest that highly expressed ENO1Ab in the maternal circulation can pass through the blood-placenta-barrier and the compromised blood-brain barrier into the brain tissues of offspring and may cause neurological development impairment mainly through complement-dependent cytotoxicity.

Keywords: anti-alpha-enolase antibody, autoimmunity, thyroiditis, brain development

Abbreviations: ADCC, antibody-dependent cell-mediated cytotoxicity; AIT, autoimmune thyroiditis; BBB, blood-brain barrier; C3, complement 3; CDC, complement-dependent cytotoxicity; CON group, control group; EAT, experimental autoimmune thyroiditis; ELISA, enzyme-linked immunosorbent assay; ENO1, alpha-enolase; ENO1Ab, specific autoantibody against alpha-enolase; f-EPSPs, field excitatory postsynaptic potentials; HE, hashimoto encephalopathy; H-ENO1Ab, high serum level of specific autoantibody against alpha-enolase; HRP, horseradish peroxidase; IF, immunofluorescence; LTP, long-term potentiation; MAC, membrane attack complex; MWM, morris water maze; PBS, phosphate-buffered saline; RT, room temperature; TEM, transmission electron microscopy; Tg, thyroglobulin; TJ, tight junction; TMB, tetramethyl-benzidine solution; TSH, thyroid-stimulating hormone; TT4, total thyroxine; TUNEL, transferase-mediated dUTP nick end-labelling; (sICAM)-1, soluble intercellular adhesion molecule-1.

Introduction

Alpha-enolase (ENO1) is a multifunctional protein that plays a role in glycolysis, autoimmunity, fibrinolysis, cell proliferation, and apoptosis [1, 2]. Upregulated expression of ENO1 on the cell membrane acts as an important autoantigen in several infectious and chronic autoimmune diseases [3]. Some studies have identified that the serum level of specific autoantibody against ENO1 (ENO1Ab) is increased in those patients with systemic lupus erythematosus, rheumatoid arthritis, and lupus nephritis [4–7]. In addition, ENO1 has been studied in some neurological disorders, such as Alzheimer's disease, encephalopathy associated with autoimmune thyroiditis (AIT), and cerebrovascular diseases [8–11]. These findings indicate that ENO1Ab may play an important role in neurological impairment.

AIT can cause not only thyroid destruction but also some extrathyroidal impairments. AIT-related brain damage includes encephalopathy in adult AIT patients (i.e., Hashimoto

encephalopathy, HE) and delayed brain development in the offspring of pregnant women with AIT, which is gaining more and more attention from immunologists, neurologists and endocrinologists [12, 13]. We have recently found that serum autoantibodies against protein disulfide isomerase A3 and the epitope aa168-183 of ENO1 expression are independently associated with thyroid autoimmunity-related miscarriage [14, 15]. The serum expression of ENO1Ab has been found to be significantly increased in both patients with HE [16] and the experimental AIT (EAT) mouse model induced by only murine thyroglobulin (mTg) immunization [17]. It was found that adult mice with high serum level of ENO1Ab (H-ENO1Ab) suffered brain damage in our previous study. Although brain development in the offspring of euthyroid women with AIT is adversely affected [12], the relevant mechanisms are not yet clear. In the present study, we first investigated whether maternal H-ENO1Ab caused brain damage in offspring, and how it was involved.

Materials and methods

Animals

Five-week-old female mice were purchased from HFK Biotech Co. Ltd. (Beijing, China). Animals were fed and mated in the specific pathogen-free animal facility at China Medical University.

Immunization and mating protocols

To assess the effects of highly expressed ENO1Ab in the maternal serum on the brain development of offspring, a pregnant H-ENO1Ab mouse model was established as depicted in our previous study [17]. The female mice were randomly separated into the two following groups. H-ENO1Ab group received ENO1 protein immunization twice with a 2-week interval while the control (CON) group received only vehicle injection twice. Four weeks after the final immunization, all female mice were drawn for blood collection and ENO1Ab detection before they were mated with intact 10-week-old CBA/J male mice. The day when vaginal plugs were first found was recorded as day 0 of pregnancy (E0). Some pregnant mice were randomly chosen and euthanized on postnatal day (P0) (*n* = 6/group), and the remaining dams were euthanized after weaning. The pups were randomly chosen and euthanized on postnatal Days P10 (*n* = 14-19/group) and P40 (*n* = 19-20/group), respectively (Fig. 1).

Enzyme-linked immunosorbent assay

Euthyroidism is very important for maintaining normal brain development in the offspring. In our previous study, ENO1-immunized adult mice showed high serum TgAb and thyroid-stimulating hormone (TSH) levels, but they did not appear until the 10th and 14th weeks after the last immunization, respectively [17]. Serum total thyroxine (TT4), TSH and TgAb levels were tested by enzyme-linked immunosorbent assay (ELISA) as previously reported [18]. The detection of serum TT4 and TSH were completed as instructed by the manufacturer (Cloud-Clone, Wuhan, China). In addition, ENO1Ab and its IgG subtypes in amniotic fluid and serum samples were measured together with serum TgAb by ELISA as described in our previous study with slight modification [17, 19].

The 96-well plates for ELISA were coated with mTg (1 μg/well) at 4°C overnight, and blocked with 1% bovine serum albumin (BSA; Sigma, USA) in phosphate-buffered saline (PBS). The serum samples were diluted at 1:50 for TgAb test, placed into the above plates, and incubated for 2 h at room temperature (RT). Amniotic fluid (not diluted) and serum samples (1:1000 diluted for dams, 1:50 diluted for pups) were put into the 96-well plates, which had been coated with ENO1 (1 μg/well) at 4°C overnight and blocked with BSA-PBS as above. After 2 h incubation at RT followed by repeated washing, the plates were further incubated with diluted horseradish peroxidase (HRP)-labeled goat anti-mouse total IgG (1:200 diluted for TgAb;1:10 000 for ENO1Ab), IgG1(1:1000 for ENO1Ab), IgG2a (1:1000 for ENO1Ab), IgG2b (1:1000 for ENO1Ab), or IgG3 antibodies (1:1000 for ENO1Ab), which were all from Bethyl (USA). 3,3′,5,5′ Tetramethyl-benzidine solution (TMB; BBI, China) and 2 mol/L hydrochloric acid were used in the chromogenic substrate reaction. The absorbance values were immediately analyzed with Infinite 2000 PRO (TECAN, Australia) at 450 nm.

Morris water maze

Morris water maze (MWM) tests were applied to evaluate the spatial cognitive development of pups on P40, as previously depicted [19, 20]. On the first day, pups swam to accommodate the water maze and platform for 120 s. Over the next 4 days, the time required for the pups to discover the platform (escape latency) was recorded. If the platform was not discovered, a latency of 120 s was recorded. On the last day, the platform was removed, and the time to reach the original position of the platform and the number of platform area crossings were recorded.

Long-term potentiation

Long-term potentiation (LTP) tests were performed as previously described [17]. The brain tissues were cut into horizontal slices (300-400 μm). All the slices available were equilibrated for 1 h in warm artificial cerebrospinal fluid continuously bubbled with 95% O_2/5% CO_2. At the beginning of each experiment, baseline levels were recorded for 10 min

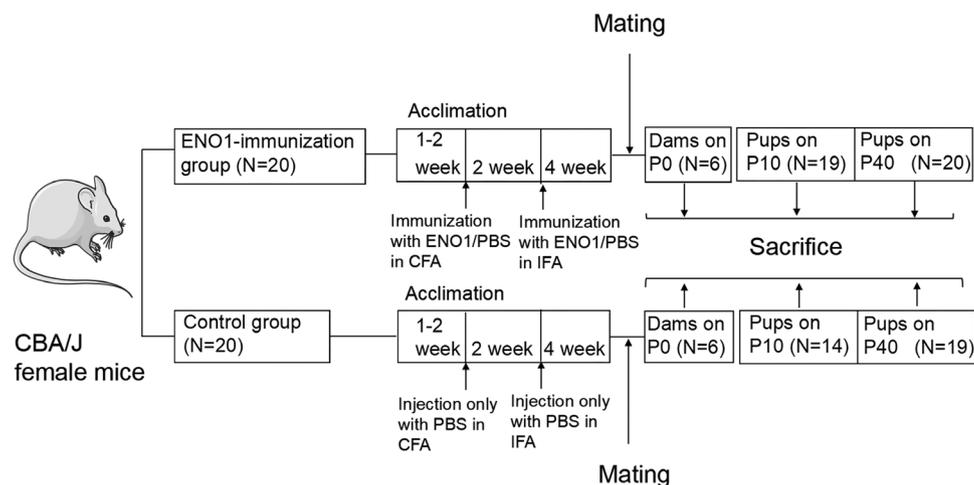**Figure 1:** research design. Each female mouse was immunized twice with 100 μg recombinant ENO1 protein in Freund's adjuvant to establish a mouse model with a high serum anti-ENO1 antibody (H-ENO1Ab) level. The control female mice were only s.c. injected with an equivalent volume of PBS in replacement of ENO1 protein. Some of the pups were examined for learning and memory abilities using the Morris water maze (MWM) test before they were sacrificed on P40.

and input/output curves were determined by increasing the intensity of the stimulus and adjusting it to elicit 70% of the maximal response. After baseline recording, field excitatory postsynaptic potentials (f-EPSPs) were measured by an MED64 planar microelectrode matrix recording system (Alpha MED Scientific, Osaka, Japan). LTP was induced and recorded for 60 min. The results were normalized as the f-EPSP slope (% of baseline).

Nissl staining and transmission electron microscopy

Whole brain tissues were removed from some pups, which were chosen at random and sacrificed on P10 (n = 8/group) and P40 (n = 8/group), respectively. These brain tissues were immediately submerged into 4% paraformaldehyde at 4 °C for 48 h. Then, they were cut into 10 μm thick slices and stored at –20 °C. The frozen sections were taken to RT for 30 min before use. They were immersed in 1% toluidine blue solution for 15 min, and were observed by a light microscope (Olympus, BX51) after dehydration, vitrification. and sealing [21].

Transmission electron microscopy (TEM) was used to evaluate the ultrastructure of the blood–brain barrier (BBB) [22, 23]. Some pups were chosen at random and anaesthetized on P10 and P40, respectively. Their brain tissues were immediately separated, cut into 1.0 mm³ specimens, and submerged in 2.5% glutaraldehyde at 4°C for 2 h. These samples were washed with deionized water, and fixed with 1% osmic acid at 4°C for 2 h. After dehydration, 70-nm-thick slices were doubly stained with lead citrate for 10 min and uranyl acetate for 20 min, and then the images were collected under TEM (H-7000, Hitachi, Japan).

Immunofluorescence staining

The frozen brain sections were prepared as described above. After blocking with 5% BSA, the slices were incubated with the following primary antibodies at 4°C overnight: rabbit antibodies against ENO1 (1:500, BIOSS, China), NeuN (1:500, Abcam, MA), rat antibodies against CD34 (1:50, Abcam), rabbit anti-C3 antibodies (1:50, Abcam), rabbit anti-CD16 antibodies (1:200, BIOSS), mouse anti-C5b-9 antibodies (1:300, CST, MA), and rabbit anti-cleaved caspase-3 (1:400, CST). Then, the slices were incubated with the following secondary antibodies: FITC-conjugated goat anti-mouse IgG (1:50, Abcam), TRITC-conjugated goat anti-rat IgG (1:50, Proteintech, MA), goat anti-rabbit IgG conjugated to Alexa Fluor 488 (1:200, Proteintech), and goat anti-rabbit IgG conjugated to Coralite 594 (1:100, Proteintech). Nuclei were counterstained with DAPI, and Leica DMi8 and SP5 (Leica, Germany) were used to observe the staining.

Western blot

Some offspring were chosen at random and sacrificed on P10 (n = 4/group), and P40 (n = 4/group), respectively. Fresh brain tissues were dissected, and the bilateral hippocampus and cortex were separated. In addition, one intact female mouse was mated with one male mouse, and the brain tissues of the pups were collected for the detection of ENO1 protein expression on embryonic Day 13 (E13), P10, P21, and P40, respectively. According to the instruction of the total protein extraction kit (KeyGen, China), all the above tissues were homogenized by shaking, and centrifuged at

12 000 × g at 4°C for 15 min, and the supernatant was collected on ice. Protein concentrations were determined using a BCA protein assay kit (Beyotime, China) [24]. The prepared protein samples were electrophoresed, and then transferred to PVDF membranes (Millipore, MA). The membranes were incubated at 4°C overnight with the following primary antibodies: rabbit anti-ENO1 antibodies (1:400, BIOSS), rabbit anti-Iba-1 antibodies (1:1000, Abcam), mouse anti-GFAP antibodies (1:1000, CST), rabbit anti-cleaved caspase-3 antibodies (1:1000, CST), rabbit anti-BDNF antibodies (1:500, Wanleibio, China), and rabbit anti-beta-actin antibodies (1:5000, BIOSS). After washing, the membranes were incubated with HRP-conjugated goat anti-rabbit IgG or goat anti-mouse IgG antibodies (1:5000, Zhongshan Golden Bridge, China). All bands were detected by the Alpha Innotech chemiluminescent darkroom system (Alpha Innotech CO., CA).

TUNEL staining

All experimental protocols for transferase-mediated dUTP nick end-labeling (TUNEL) staining were conducted according to the instruction of In Situ Cell Death Detection Kit (Roche, Switzerland) [25]. After fixation with 4% paraformaldehyde, blocking with 3% H_2O_2 in methanol and permeabilizing with 0.1% sodium citrate containing 0.1% Triton X-100, the tissue sections were incubated with terminal deoxynucleotidyl transferase and dUTP at 37°C for 1 h. Then, they were counterstained with DAPI at RT for 3 min and observed under Leica SP5 (Leica). TUNEL-positive cells were counted using ImageJ.

Microarray

Whole-brain homogenates from the pups on P10 (n = 2/group) were prepared as depicted in our previous study [25]. Forty cytokines in the supernatants were quantified by a Proteome Profiler Mouse Cytokine Array Kit (R&D Systems, Minneapolis, MN, USA).

Statistical analysis

SPSS software (version 23.0, IBM Corporation, NY, USA) was used to perform all statistical analyses. Statistical significance between groups was measured by independent samples t tests or Mann–Whitney U tests. Data are reported as the mean ± SEM. Statistical significance was defined as $P < 0.05$.

Results

ENO1Ab levels in maternal mice and their offspring

To confirm that the female H-ENO1Ab mouse model was successfully established and to explore whether maternal ENO1Ab can penetrate the blood-placental barrier into the offspring, serum and amniotic fluid ENO1Ab levels were measured. Serum ENO1Ab was significantly increased in ENO1-immunized dams at pre-pregnancy and in their pups on P10 and P40 when compared with the control group of dams and their offspring, respectively. Serum ENO1-specific IgG1 and IgG2a levels in the pups of ENO1-immunized dams were markedly increased on P10 and P40, but IgG2b and IgG3 levels were not changed (Fig. 2A, B). Furthermore, the ENO1Ab levels were significantly higher in the amniotic fluid of ENO1-immunized dams than in that of the control group (Fig. 2A). These findings suggest the successful establishment of a pregnant H-ENO1Ab mouse model (i.e., H-ENO1Ab
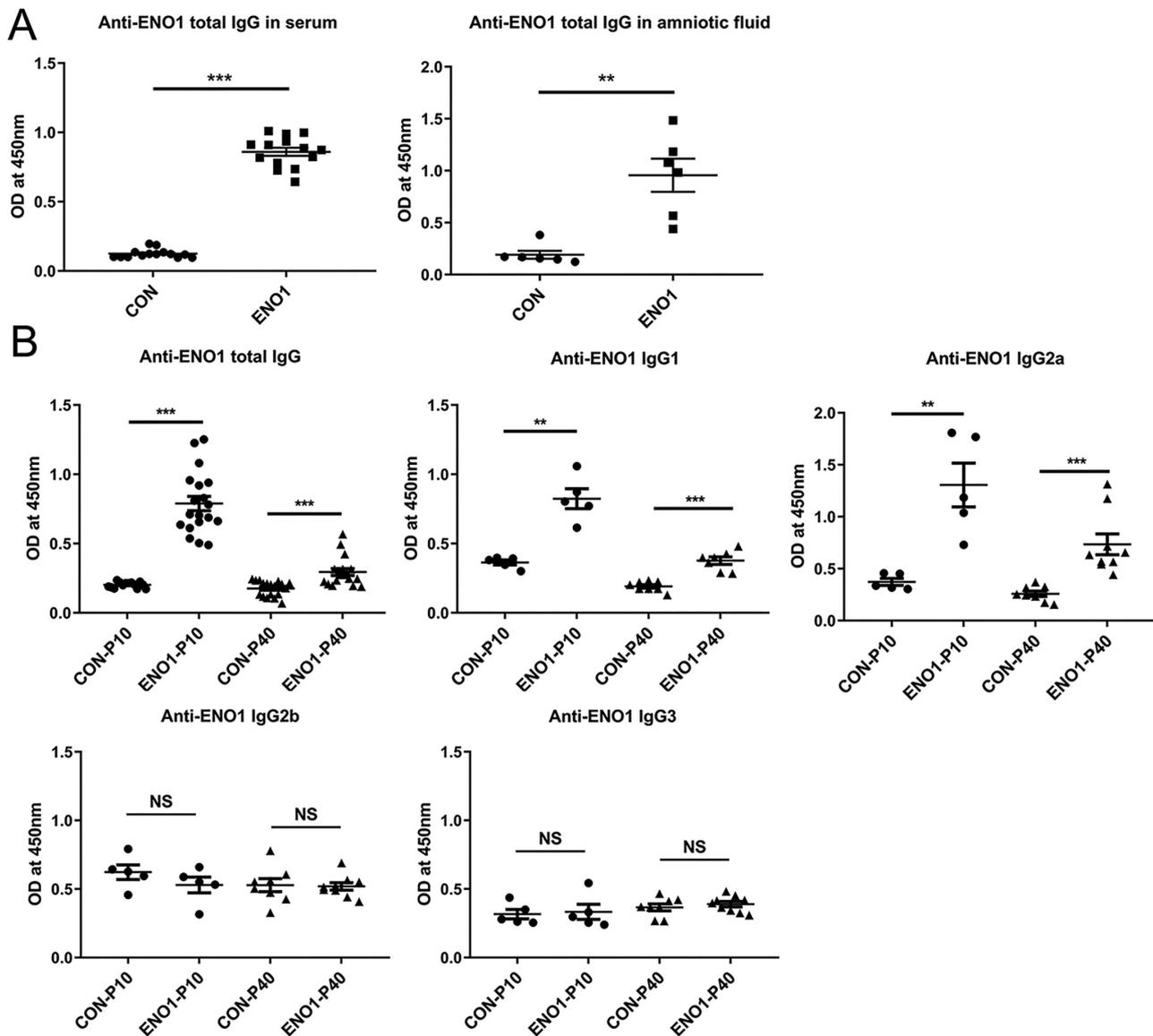
Figure 2: the levels of ENO1Ab in the H-ENO1Ab dams and their pups. Serum and amniotic fluid samples were collected as depicted in Fig. 1. Anti-ENO1 total IgG and its subtypes were measured by enzyme-linked immunosorbent assay (ELISA). The results are shown above for the dams (A, n = 6-14/group, **P < 0.01, ***P < 0.001 vs. the control group) and the pups (B, n = 14-19 for total IgG, n = 5-8 for IgG1, n = 5-9 for IgG2a, IgG2b and IgG3, **P < 0.01, ***P < 0.001, not significantly (NS) vs. the pups of the control group).

dam model) and the transmission of ENO1-specific IgG from dams to pups through the placental barrier.

Assessment of learning and memory abilities

The MWM test was used to assess the learning and memory abilities of the pups on P40. The pups of H-ENO1Ab dams showed pronouncedly longer escape latencies than those of the CON group (Fig. 3A). Furthermore, the average f-EPSP slopes and the amplitude changes after high-frequency stimulation were decreased in the P40 pups of H-ENO1Ab dams as compared with those of the CON group in the LTP test (Fig. 3B). These findings indicate that learning and memory abilities may be damaged in the offspring of H-ENO1Ab females.

Serum TSH, TT4, and TgAb levels in offspring

In our previous study, none of serum TgAb, TSH, and TT4 levels were significantly changed in H-ENO1Ab mice before the 10th week after the second challenge of ENO1 protein

[17]. In this study, all the dams had delivered before the 8th week after the last immunization. Therefore, the thyroid dysfunction and TgAb production developed later in the H-ENO1Ab dams were not the pathogenic factors for the above neurological damage in their pups. Moreover, there were no significant differences in serum TT4, TSH, or TgAb levels between the pups of H-ENO1Ab dams and those of the CON group on P10 and P40 (Fig. 4), which did not contribute to the decreased learning and memory abilities, either.

ENO1 expression in the brain tissue

ENO1 protein is widely expressed in the neurons, microglia, astrocytes, and vascular endothelial cells of mature brain tissue [17]. The expression of ENO1 protein in the brain tissues of the offspring was further measured by western blot, and its presence was found on E13, P10, P21, and P40 (Fig. 5). This suggests that ENO1Ab transferred from dams may
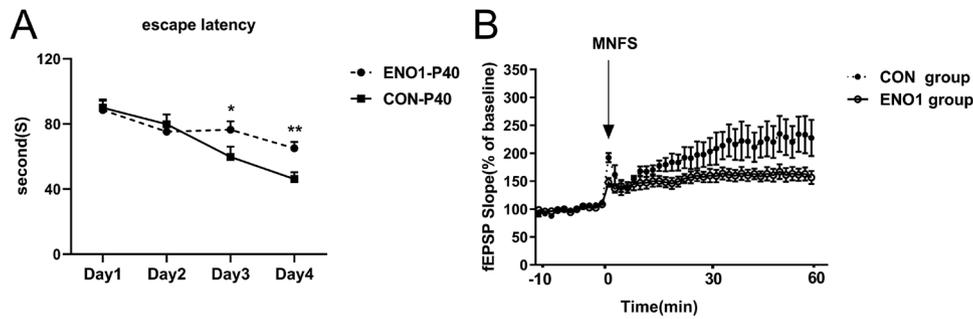
Figure 3: MWM and long-term potentiation tests in the pups of the H-ENO1Ab dams on P40. All the pups were obtained as depicted in Fig. 1. (A) MWM tests of learning and memory abilities via the assessment of escape latency in the pups from H-ENO1Ab dams (*n* = 20) and the control group (*n* = 19) on P40. (B) Long-term potentiation (LTP) was expressed as f-EPSP% after high-frequency stimulation in the pups from H-ENO1Ab dams (*n* = 6) and those from the control group (*n* = 5) on P40. $^*P < 0.05$, $^{**}P < 0.01$ vs. the pups of the control group.
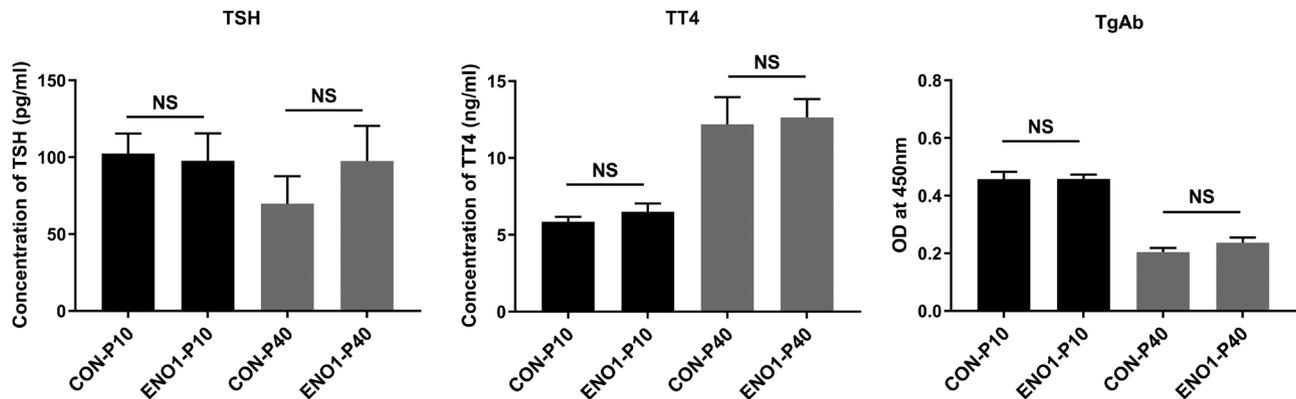

Figure 4: the examination of thyroid functions and serum TgAb in the pups of H-ENO1Ab dams. All the pups were obtained as depicted in Fig. 1. Serum levels of TSH, TT4, and TgAb were detected by ELISA in the pups of H-ENO1Ab dams on P10 (*n* = 5-9/group) and P40 (*n* = 8-9/group. NS, vs. the pups of the control group).
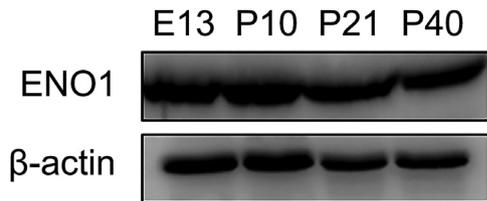

Figure 5: detection of ENO1 protein expression in the brain tissues of the pups by western blot. One intact female mouse was mated with one male mouse, and the brain tissues of the pups were obtained for the detection of ENO1 protein expression on E13, P10, P21, and P40.

cause brain damage in the offspring due to ENO1 protein expression at the early life stage.

Histopathological alteration in the brain tissue

Nissl staining was used to observe morphological alterations in the brain tissues of the pups. Obvious vacuolar degeneration and irregular cell alignment were found in extracortical granular layer cells of the pups from H-ENO1Ab dams on P10 (Fig. 6). The tight junction (TJ) is the fundamental structure of BBB [26]. TJs seemed to be damaged in pups of H-ENO1Ab dams on P10 and P40 under TEM (Fig. 7). TJ injury had been demonstrated in H-ENO1Ab adult mice in our previous study [17]. This suggests that ENO1Ab may cause neurological damage by destroying the integrity of TJs.

ENO1Ab-mediated immune attack on brain tissue in offspring

At the early life stage, IgG can pass the incomplete BBB [27]. In addition, TJs seemed to be damaged in the offspring of H-ENO1Ab dams. Therefore, immunofluorescence (IF) staining was performed on the brain tissue sections to explore whether IgG entered the central nervous system of pups and caused immune attack. IgG deposits were evident in the brain tissues of the pups from H-ENO1Ab dams on P10 and modest on P40, whereas they were barely present in those from the CON group at both time points (Fig. 8A). Furthermore, IgG deposits were found mainly on the surface of neurons (NeuN+) and vascular endothelial cells (CD34+), which colocalized with the ENO1 protein (Fig. 8B). Both the colocalized complement 3 (C3) with IgG (Fig. 8C) and membrane attack complex (MAC, Fig. 8D) were obviously detectable in the brain tissue of the pups from H-ENO1Ab dams, but no CD16+ cell aggregation was found in the IgG deposit sites (Fig. 8E). IF staining and western blot examination showed obviously elevated cleaved caspase-3 expression in the cortical and hippocampal tissues of the pups from H-ENO1Ab dams on P10 (Fig. 9A, B). The TUNEL assay also showed consistent findings in cell apoptosis with caspase-3 expression detection. The percentage of TUNEL-positive cells was markedly increased in the brain tissues of pups from H-ENO1Ab dams as compared with those from the CON group on P10 (Fig. 9C, D).
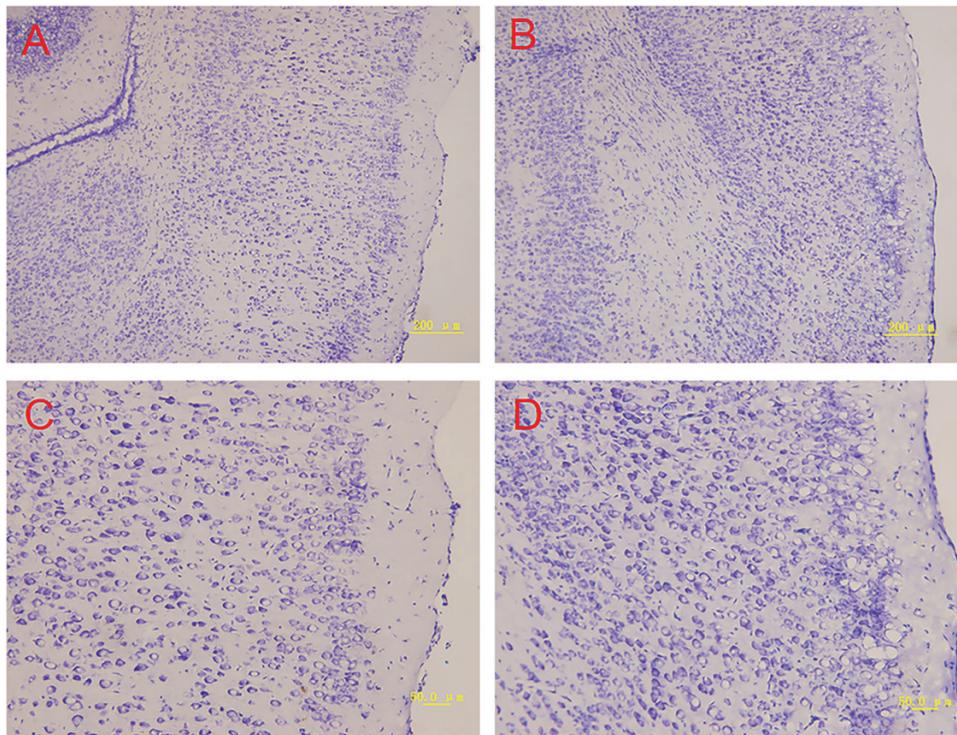
Figure 6: Nissl staining of brain tissues in the pups of H-ENO1Ab dams on P10. All the pups were obtained as depicted in Fig. 1. Nissl staining was performed on brain tissue slices from the pups of the control group (A, C; *n* = 6) and those of the H-ENO1Ab dams (B, D; *n* = 6) and observed under a light microscope (A and B, ×100; C and D, ×200).

Microglia and astrocytes in the hippocampus and cortex tissues were quantitatively examined by Western blot. The levels of both Iba-1 (marker for microglia) and GFAP (marker for astrocytes) were significantly increased in the hippocampal and cortical tissues of the pups from H-ENO1Ab dams on P10, but only upregulation of Iba-1 expression was found in the cortex on P40 when compared with those of the CON group (Fig. 10A, B). The results indicate that the two kinds of glial cells presented proliferative responses to the infusion of ENO1Ab into the brain tissue. Multiple cytokine expressions were assessed in the brain homogenates of the pups from H-ENO1Ab dams by cytokine panel microarrays. However, only soluble intercellular adhesion molecule (sICAM)-1 seemed to be increased by more than 50% in the pups from H-ENO1Ab dams as compared with those from the CON group in the two repeated experiments with consistent results (Fig. 10C). The expression levels of proinflammatory cytokines, such as IFN-γ, IL-1β, IL-6, and TNF-α, were not obviously altered in the pups of H-ENO1Ab dams. These findings indicate that microglia and astrocytes may not be overtly activated, although they show proliferation, or that M2-type microglia may prevail. The level of BDNF in the brain homogenates was further determined by western blotting. It was found that the expression of BDNF was higher in the pups from H-ENO1Ab dams when compared with that of the pups from the CON group on P10 (Fig. 10D). The increased BDNF production had been found with involvement in neurological repair [28].

Discussion

ENO1 is expressed on many eukaryotic cells, such as thyroid epithelial cells, neurons, and vascular endothelial cells. In our previous study on the occurrence of miscarriage related to thyroid autoimmunity, we identified abortion-related ENO1 epitopes which specific autoantibodies were significantly higher in euthyroid females with thyroid autoimmunity than healthy controls [15]. To assess the effects of maternal ENO1Ab on the brain development of offspring, a pregnant H-ENO1Ab mouse model was established in ENO1-immunized female mice after mating with intact males. Their offspring were tested for brain development on P10 (equivalent to human newborns) and P40 (equivalent to human adolescents) [29]. The two time-points (P10 and P40) had been selected to investigate the influences of some non-genetic factors (e.g. maternal TgAb and hypoxia-ischaemia) on the brain development of the offspring in those previous studies using mouse models [18, 30].

Brain development was mainly assessed by examining learning, memory and spatial exploration abilities on P40 through the MWM test. The latter is divided into two parts: directional navigation and space exploration. The former is controlled by the hippocampus, inner olfactory cortex and pericortex structures, and the latter is controlled by the dorsal striatum and connective structures [31]. The hippocampus has long been recognized as a key structure for cognitive formation. The primary sensory cortex is considered as a stimulus receptor for learning memory [32]. Both a reduction in the cortical neuron number and loss of functional structure can affect normal cognition. In the present study, the MWM test was performed in the P40 pups of H-ENO1Ab dams. They showed a significantly prolonged escape latency on days 4 and 5 of training when compared with those of the CON group. These findings demonstrate that the learning and memory capabilities of the offspring from females with high ENO1Ab expression may be impaired.
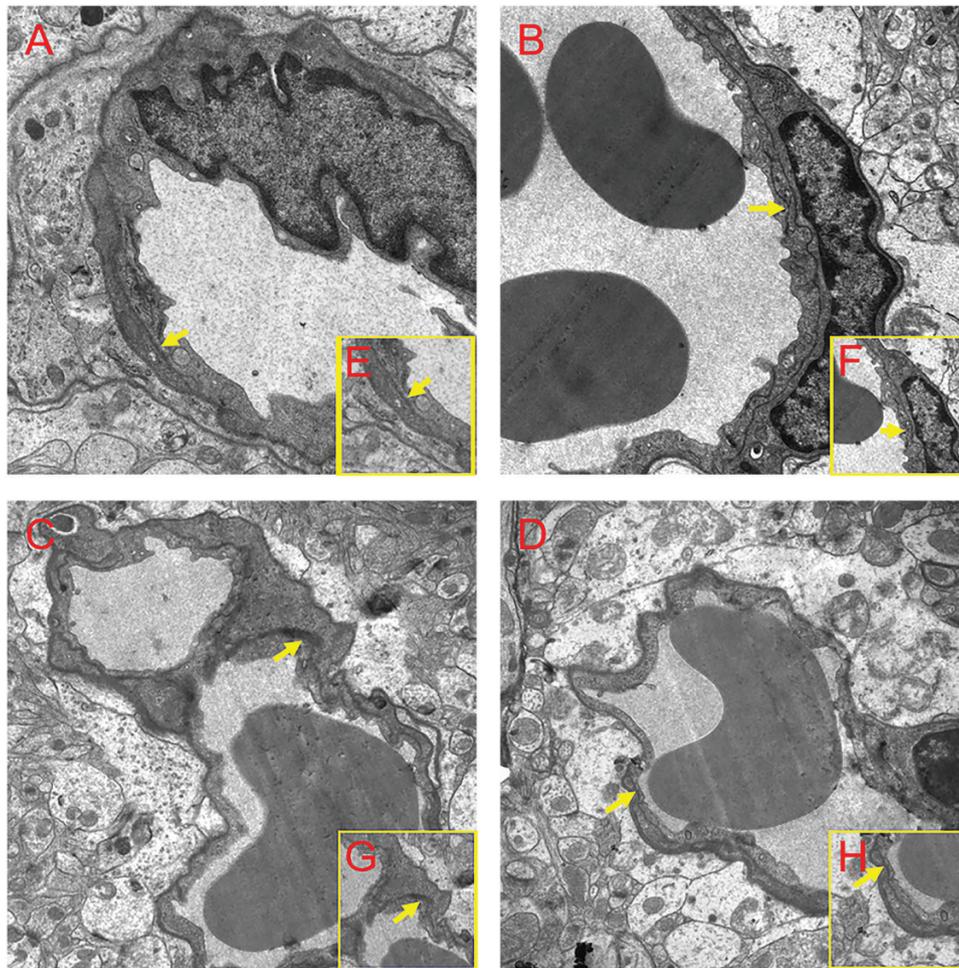
Figure 7: observation of the brain tissue ultrastructure in the pups of H-ENO1Ab dams. All the pups were obtained as depicted in Fig. 1. Transmission electron microscopic images of representative ultrastructure in the brain tissue from the pups of the control (A and C, ×15 000; E and G, ×30 000) and H-ENO1Ab dams (B and D, ×15 000; F and H, ×30 000) on P10 (A, B, E, and F) and P40 (C, D, G, and H). Yellow arrows indicate tight junctions.

ENO1 has been found to be an important autoantigen in some autoimmune diseases, and almost all ENO1Abs have been reported to be IgG-type autoantibodies [33]. IgG can cross the placental barrier into offspring [34]. The ENO1Ab level in the amniotic fluid was significantly increased in H-ENO1Ab dams when compared with that of the control pregnant mice. Moreover, serum ENO1Ab levels were pronouncedly increased in the pups of H-ENO1Ab dams, which showed a gradually decreasing trend with age. These results indicate that ENO1Ab in the pups came from their mothers. In this study, the microvascular ultrastructure in the brain tissue of the pups from H-ENO1Ab dams was observed by TEM, and the TJs seemed to be thinner than those of the pups from the CON group. This suggests that the BBB may be damaged by ENO1Ab, which has been previously found in adult mice [17]. Furthermore, the fetal BBB can allow IgG to pass through, which is different from the adult one [27]. These mechanisms together with cerebral expression of ENO1 protein at the early life stage may be responsible for the IgG deposition within the brains of H-ENO1Ab females' offspring. It can explain why IgG deposits were mainly localized on the neurons and vascular endothelial cells in the brains of pups in this study, while IgG was only found on the vascular endothelium but not on the neurons in our previous study with adult mice [17].

Although some complement proteins are likely to enter the brain tissue when the integrity of the BBB is compromised [35, 36], the complement components in the brain tissue are mainly generated by local astrocytes and microglia in response to injury. Moreover, brain cells can produce complement proteins in early pregnancy [35]. The activation of C3 can lead to either phylactic or harmful effects on the brain [37]. In this study, the production of C3 and the formation of MAC were examined since IgG entered and deposited in the parenchyma of the brain. Both colocalized C3 with IgG and MAC were obviously detectable in the brain tissues of the pups from H-ENO1Ab dams, but no CD16+ cell aggregation was found in the IgG deposit sites. CD16 is an activated receptor for the IgG Fc fragment, which can cause antibody-dependent cell-mediated cytotoxicity (ADCC) [38]. Our previous study has found that IgG2a and IgG1 were the two major subclasses of ENO1Ab produced in ENO1-immunized adult mice [17]. These results suggest that IgG against ENO1 may pass through the BBB and cause damage of neurons and vascular endothelial cells by complement-dependent cytotoxicity (CDC) rather than ADCC. CDC can cause both cell lysis and apoptosis [39]. TUNEL, caspase-3 detection and Nissl staining demonstrated damage of brain cells in the pups from H-ENO1Ab dams on P10, which further showed the impaired learning and memory abilities on P40. This suggests
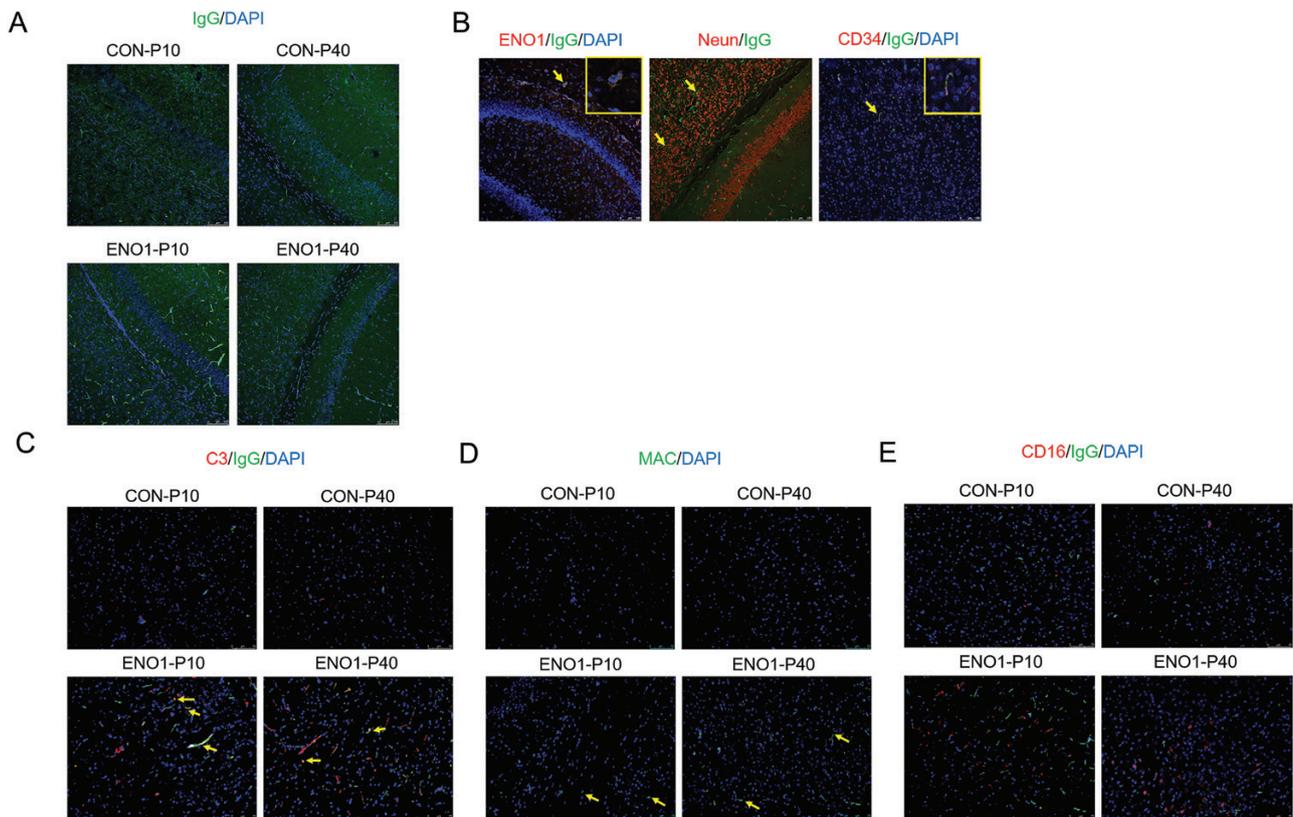
Figure 8: IgG deposition and the distribution of C3, MAC, and CD16 in the brain tissue of the pups from H-ENO1Ab dams. All the pups were obtained as depicted in Fig. 1. (A) Representative images of IgG deposition in the brain tissues from the pups of H-ENO1Ab dams and those of the control group on P10 and P40 (n = 4/group) after immunofluorescence (IF) staining with FITC-conjugated goat anti-mouse IgG (green, ×200). (B) Representative images for the colocalization of IgG and ENO1, NeuN, and CD34 in the brain tissues from the pups of H-ENO1Ab dams and those of the control group on P10 (n = 4/group) after double IF staining with FITC-conjugated goat anti-mouse IgG (green) and rabbit anti-ENO1 and NeuN, rat anti-CD34 (red, ×200). (C and E) Representative images of the colocalization of IgG and C3 and CD16 in the brain tissues from the pups of H-ENO1Ab dams and those of the control group on P10 and P40 (n = 4/group) after double IF staining with FITC-conjugated goat anti-mouse IgG (green) and rabbit anti-C3 and CD16 (red, ×200). (D) Representative images of MAC expression in the brain tissues from the pups of H-ENO1Ab dams and the those of the control group on P10 and P40 (n = 4/group) after IF staining with mouse anti-C5b-9 (green, ×200). Nuclei were counterstained with DAPI (blue).

that prenatal exposure to ENO1Ab can adversely affect intellectual development until adolescence.

The increased microvascular permeability causes harmful circulatory substances to enter the central nervous system through the BBB, which may activate glial cells to release pro- and anti-inflammatory cytokines and neurotrophic factors [40, 41]. Astrocytes are important for normal neuronal development by supporting BBB integrity, synapse formation and neurological repair. In addition to phagocytosis and homeostasis maintenance, activated microglia may transform to M1-type (neuro-destructive microglia) and M2-type (neuro-protective microglia) ones in the lesions of the central nervous system where the BBB is disrupted. M1 can produce proinflammatory cytokines (e.g. IL-6 and TNFα), whereas M2 can produce neuroprotective factors (e.g. BDNF) [41]. The proinflammatory or anti-inflammatory effects of microglia and astrocytes are related to the mode of injury [41, 42]. In our previous study on ENO1-immunized adult mice, the BBB was not sufficiently disrupted to allow the entrance of IgG into the brain parenchyma. Although microglia and astrocytes were found with obvious increases in the brain, C3 was not detectable while only IL-6 level and Tau phosphorylation were increased in ENO1-immunized adult mice [17]. In the current study on pups from ENO1-immunized adult mice, ENO1-specific IgG passed through the BBB and deposited on

not only the vascular endothelium but also neurons. Under this stimulation, the proliferation of microglia and astrocytes led to more C3 distribution and BDNF production in the brains of the pups from H-ENO1Ab dams, but the expressions of proinflammatory cytokines, such as IFN-γ, IL-1β, IL-6, and TNF-α, were not obviously altered. These findings were different from those in the ENO1-immunized adult mice described before. It has been known that BDNF is potentially involved in neurological repair [28]. Increased BDNF production can facilitate the repair and regeneration of neurons [28]. In addition, ICAM-1 regulates the interactions between the extracellular environment and neural cells [43]. Under physiological conditions, the basal expression of sICAM-1 is weak and mostly occurs in endothelial cells, while under some pathological conditions (e.g. AD), sICAM-1 expression is more likely increased in astrocytes [44]. In this study, sICAM-1 seemed to be increased by more than 50% in the brain tissues of the pups from H-ENO1Ab dams, which potentially further contributed to BBB dysfunction and neuroinflammation [45].

Although euthyroidism is very important for maintaining normal brain development in offspring, it is still adversely affected in euthyroid women with AIT [12]. The relevant mechanisms are not yet clear, and isolated production of maternal TgAb is found not able to affect the brain development in offspring [18]. The expression of ENO1Ab have been
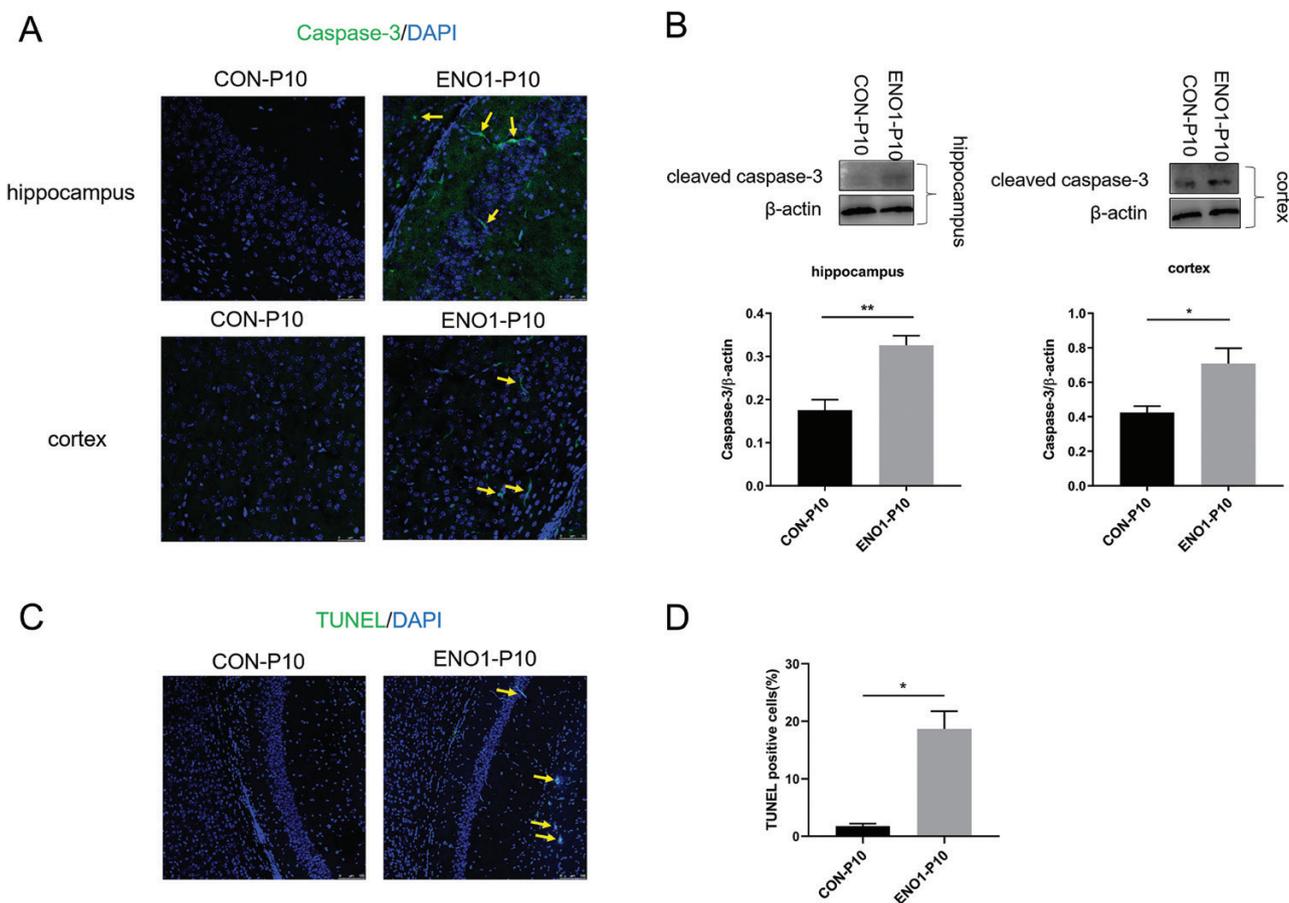
Figure 9: cleaved caspase-3 and TUNEL-positive cell distribution in the brain tissue of the pups from H-ENO1Ab dams. All the pups were obtained as depicted in Fig. 1. (A) Representative images of cell apoptosis distribution in hippocampal and cortical tissues of the pups from H-ENO1Ab dams and those of the control group on P10 ($n = 4$/group) after IF staining with rabbit anti-cleaved caspase-3 (green, ×400). Nuclei were counterstained with DAPI (blue). (B) Assessment of cleaved caspase-3 expression in hippocampal and cortical tissues of the pups from H-ENO1Ab dams and those of the control group on P10 ($n = 4$/group) was performed by western blot. $^*P < 0.05$, $^{**}P < 0.01$ vs. the pups of the control group on P10. (C) Terminal deoxyribonucleotidyl transferase-mediated dUTP nick end labelling (TUNEL) staining images of apoptotic cell detection in the brain tissues from the pups of H-ENO1Ab dams and those of the control group on P10 (green, ×200, $n = 4$/group). Nuclei were counterstained with DAPI (blue). (D) The percentage of TUNEL-positive cells in the pups of H-ENO1Ab dams and the control group on P10 ($n = 4$/group) was analysed using ImageJ. $^*P < 0.05$, $^{**}P < 0.01$ vs. the pups of the control group on P10.

found with a moderate, significant increase in EAT mice at the 4th week after the last immunization of Tg, when high serum level of TgAb and obvious intrathyroidal mononuclear infiltrates have been shown [17]. In another study from our group [18], there were no thyroid dysfunctions shown in female EAT adult mice when they were examined at 4th and 7th–8th after the last challenge of Tg. In another EAT model established in NOD mice after Tg immunization, no thyroid dysfunctions were found, either [46]. In our previous study on ENO1-immunized female adult mice, serum TgAb level and intrathyroidal mononuclear infiltrates were not significantly, moderately increased until the 10th week after the last challenge of ENO1 protein, and serum TSH concentration was not markedly up-regulated until the 14th week, while serum TT4 remained unchanged [17]. These findings indicate that the production of ENO1Ab may be secondary to the autoimmune responses against Tg, and it can further promote mononuclear cell infiltration and autoimmune attack to thyrocytes, which eventually cause thyroid dysfunctions. In the current study, all H-ENO1Ab dams had given the birth before the 8th week after the last immunization. No significant differences were found in serum TSH, TT4, or TgAb levels

between the pups of H-ENO1Ab dams and those of the CON group on both P10 and P40. Thus, maternal H-ENO1Ab is indicated as an important pathogenic factor for the brain development damage in offspring, which may exert adverse extrathyroidal effects independently on the existence of TgAb and thyroid dysfunctions. It may become a new predicative marker and interventional target for the neurological impairment in the offspring of AIT females.

There were several limitations in the present study. We did not quantify BBB permeability, although we previously and quantitatively demonstrated its increase in ENO1-immunized adult mice [17]. In addition, the related mechanisms for cerebral ENO1Ab to stimulate the production of complement proteins, sICAM-1 and BDNF need to be further investigated. We previously showed that autoantibodies against the epitope aa168–183 of ENO1 are independently associated with thyroid autoimmunity-related miscarriage [15]. The NH2-terminal region of ENO1 has been reported as a target for autoantibodies in HE [47], but the specific epitope has not been determined yet. We will further explore the specific epitopes of maternal ENO1Ab which are responsible for brain damage in offspring in the future.
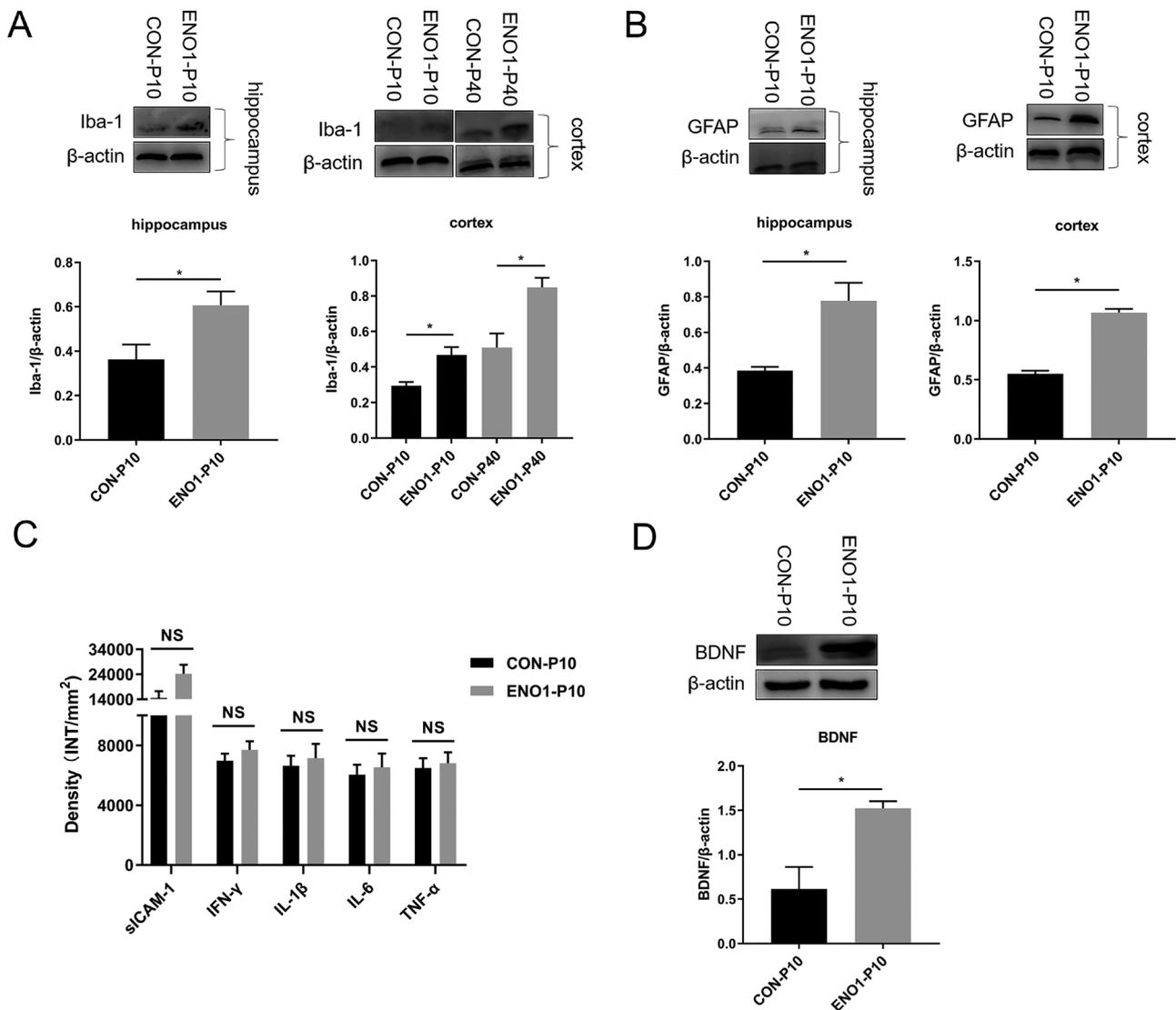
Figure 10: quantitative examination of glial cells in hippocampal and cortical tissues and assessment of cytokine and BDNF levels in the brain tissue of the pups from H-ENO1Ab dams. All the pups were obtained as depicted in Fig. 1. The expression levels of Iba-1 (A) and GFAP (B) in the hippocampal and cortical tissues from the pups of H-ENO1Ab dams and those of the control group on P10 and P40 ($n = 4$/group, respectively) were quantitatively assessed by western blot. $^*P < 0.05$ vs. the pups of the control group at the same age. (C) The average levels of cytokines in the supernatants of brain tissue homogenates from the pups of H-ENO1Ab dams and those of the control group on P10 were detected by microarray ($n = 4$/group). NS vs. the pups of the control group. (D) The levels of BDNF in the brain tissues of the pups from H-ENO1Ab dams and those of the control group on P10 ($n = 4$/group) were detected by western blot. $^*P < 0.05$ vs. the pups of the control group on P10.

Conclusions

Our results indicate that circulating maternal ENO1Ab can pass through the placenta and the compromised BBB into the central nervous system of offspring, and deposit on the surface of neurons and vascular endothelial cells, which may cause the damage of neurological development mainly through CDC. ENO1Ab is highly expressed in some AIT patients. Our previous investigation has described the potential mechanisms for the contribution of ENO1Ab to HE in adults. To the best of our knowledge, this pilot study has first reported how maternal H-ENO1Ab may adversely influence the brain development of offspring. The contributions of ENO1Ab to extrathyroidal damage are worthy of much investigation, which may help to identify new predictive biomarkers and therapeutic targets.

Acknowledgements

Ethics approval

The whole experimental programs were rigorously consistent with the Guideline for Animal Care and Use Committee and were approved by the Ethics Committee of China Medical University. The animal research adheres to the ARRIVE guidelines (https://arriveguidelines.org/arrive-guidelines).

Conflict of interests

None declared.

Data Availability

The datasets generated for this study are available on request to the corresponding author.

Author contributions

J.L., Z.S., W.T., and Y.F. designed the study. W.S., Y.F., H.L., X.H., and Y.L. conducted the experiments and analyzed the data. W.S., Y.F., and J.L. wrote the manuscript. All authors approved the final version of the manuscript.

Permission to reproduce

Not applicable.

Clinical trial registration

Not applicable.

References

1. Saulot V, Vittecoq O, Charlionet R, Fardellone P, Lange C, Marvin L, et al. Presence of autoantibodies to the glycolytic enzyme alpha-enolase in sera from patients with early rheumatoid arthritis. *Arthritis Rheum* 2002, 46, 1196–201. doi:10.1002/art.10252.
2. Cappello P, Principe M, Bulfamante S, Novelli F. Alpha-enolase (ENO1), a potential target in novel immunotherapies. *Front Biosci (Landmark Ed)* 2017, 22, 944–59. doi:10.2741/4526.
3. Didiasova M, Schaefer L, Wygrecka M. When place matters: shuttling of enolase-1 across cellular compartments. *Front Cell Dev Biol* 2019, 7, 61. doi:10.3389/fcell.2019.00061.
4. Bruschi M, Petretto A, Santucci L, Vaglio A, Pratesi F, Migliorini P, et al. Neutrophil extracellular traps protein composition is specific for patients with Lupus nephritis and includes methyl-oxidized alphaenolase (methionine sulfoxide 93). *Sci Rep* 2019, 9, 7934.
5. Bruschi M, Sinico RA, Moroni G, Pratesi F, Migliorini P, Galetti M, et al. Glomerular autoimmune multicomponents of human lupus nephritis in vivo: alpha-enolase and annexin AI. *J Am Soc Nephrol* 2014, 25, 2483–98.
6. Bae S, Kim H, Lee N, Won C, Kim HR, Hwang YI, et al. alpha-Enolase expressed on the surfaces of monocytes and macrophages induces robust synovial inflammation in rheumatoid arthritis. *J Immunol* 2012, 189, 365–72.
7. Li M, Li J, Wang J, Li Y, Yang P. Serum level of anti-a-enolase antibody in untreated systemic lupus erythematosus patients correlates with 24-hour urine protein and D-dimer. *Lupus* 2018, 27, 139–42.
8. Kanavaki A, Spengos K, Moraki M, Delaporta P, Kariyannis C, Papassotiriou I, et al. Serum levels of S100b and NSE proteins in patients with non-transfusion-dependent thalassemia as biomarkers of brain ischemia and cerebral vasculopathy. *Int J Mol Sci* 2017, 18, 2724.
9. Agoston DV, Shutes-David A, Peskind ER. Biofluid biomarkers of traumatic brain injury. *Brain Inj* 2017, 31, 1195–203.
10. Zhang CX, Zhang DJ, Wang YL, Han W, Shi GC, Zhang HQ. Expression level of NSE, S100B and NPY in children with acute miliary phthisis and secondary tubercular meningitis. *Eur Rev Med Pharmacol Sci* 2016, 20, 1474–8.
11. Butterfield DA, Lange ML. Multifunctional roles of enolase in Alzheimer's disease brain: beyond altered glucose metabolism. *J Neurochem* 2009, 111, 915–33.
12. Li Y, Shan Z, Teng W, Yu X, Li Y, Fan C, et al. Abnormalities of maternal thyroid function during pregnancy affect neuropsychological development of their children at 25-30 months. *Clin Endocrinol (Oxf)* 2010, 72, 825–9.
13. Tamagno G, Gaoatswe G. Time for the endocrinologists to expand their awareness of and contribution to the diagnosis and management of encephalopathy associated with autoimmune thyroid disease. *Hormones (Athens)* 2011, 10, 36–8.
14. Yang Z, Wang H, Liu Y, Feng Y, Xiang Y, Li J, et al. The expression of anti-protein disulfide isomerase A3 autoantibody is associated with the increased risk of miscarriage in euthyroid women with thyroid autoimmunity. *Int Immunopharmacol* 2022, 104, 108507.
15. He X, Liu Y, Wang H, Sun W, Lu Y, Shan Z, et al. A predictive role of autoantibodies against the epitope aa168-183 of ENO1 in the occurrence of miscarriage related to thyroid autoimmunity. *Front Immunol* 2022, 13, 890502.
16. Yoneda M, Fujii A, Ito A, Yokoyama H, Nakagawa H, Kuriyama M. High prevalence of serum autoantibodies against the amino terminal of alpha-enolase in Hashimoto's encephalopathy. *J Neuroimmunol* 2007, 185, 195–200.
17. Lu Y, Qin J, Xiang Y, Sun R, Feng Y, Zhang H, et al. Experimental evidence for alpha enolase as one potential autoantigen in the pathogenesis of both autoimmune thyroiditis and its related encephalopathy. *Int Immunopharmacol* 2020, 85, 106563.
18. Wang X, Liu H, Zhang Y, Li J, Teng X, Liu A, et al. Effects of isolated positive maternal thyroglobulin antibodies on brain development of offspring in an experimental autoimmune thyroiditis model. *Thyroid* 2015, 25, 551–8.
19. Xiang Y, Jin Q, Li L, Yang Y, Zhang H, Liu M, et al. Physiological low-dose oestrogen promotes the development of experimental autoimmune thyroiditis through the up-regulation of Th1/Th17 responses. *J Reprod Immunol* 2018, 126, 23–31.
20. Wang S, Teng W, Gao Y, Fan C, Zhang H, Shan Z. Early levothyroxine treatment on maternal subclinical hypothyroidism improves spatial learning of offspring in rats. *J Neuroendocrinol* 2012, 24, 841–8.
21. Gu JX, Cheng XJ, Luo X, Yang X, Pang YP, Zhang XF, et al. Luteolin ameliorates cognitive impairments by suppressing the expression of inflammatory cytokines and enhancing synapse-associated proteins GAP-43 and SYN levels in streptozotocin-induced diabetic rats. *Neurochem Res* 2018, 43, 1905–13.
22. Gao X, Wang YC, Liu Y, Yue Q, Liu Z, Ke M, et al. Nanoagonist-mediated endothelial tight junction opening: A strategy for safely increasing brain drug delivery in mice. *J Cereb Blood Flow Metab* 2017, 37, 1410–1424.
23. Chen ZX, Li B, Liu T, Wang X, Zhu Y, Wang L, et al. Evaluation of paeonol-loaded transethosomes as transdermal delivery carriers. *Eur J Pharm Sci* 2017, 99, 240–5.
24. Qin J, Li L, Jin Q, Guo D, Liu M, Fan C, et al. Estrogen receptor beta activation stimulates the development of experimental autoimmune thyroiditis through up-regulation of Th17-type responses. *Clin Immunol* 2018, 190, 41–52.
25. Yang W, Xiang Y, Zhang H, Shan Z, Li J, Teng W. The role of protein disulphide-isomerase A3 as autoantigen in the pathogenesis of autoimmune thyroiditis and related brain damage in adult mice. *Clinical Immunology*, 2020, 212, 108350.
26. Kaya M, Ahishali B. Basic physiology of the blood-brain barrier in health and disease: a brief overview. *Tissue Barriers* 2021, 9, 1840913.
27. Diamond B, Huerta PT, Mina-Osorio P, Kowal C, Volpe BT. Losing your nerves? Maybe it's the antibodies. *Nat Rev Immunol* 2009, 9, 449–56.
28. Gordon T. The physiology of neural injury and regeneration: the role of neurotrophic factors. *J Commun Disord* 2010, 43, 265–73.
29. Dutta S, Sengupta P. Men and mice: relating their ages. *Life Sci* 2016, 152, 244–8.

30. Goffigan-Holmes J, Sanabria D, Diaz J, Flock D, Chavez-Valdez R. Calbindin-1 expression in the hippocampus following neonatal hypoxia-ischemia and therapeutic hypothermia and deficits in spatial memory. *Dev Neurosci* 2019, 12, 1–15.

31. Vorhees CV, Williams MT. Assessing spatial learning and memory in rodents. *ILAR J* 2014, 55, 310–32.

32. Weinberger NM. New perspectives on the auditory cortex: learning and memory. *Handb Clin Neurol* 2015, 129, 117–47.

33. Terrier B, Degand N, Guilpain P, Servettaz A, Guillevin L, Mouthon L. Alpha-enolase: a target of antibodies in infectious and autoimmune diseases. *Autoimmun Rev* 2007, 6, 176–82.

34. Patel DD, Bussel JB. Neonatal Fc receptor in human immunity: Function and role in therapeutic intervention. *J Allergy Clin Immunol* 2020, 146, 467–78.

35. Veerhuis R, Nielsen HM, Tenner AJ. Complement in the brain. *Mol Immunol* 2011, 48, 1592–603.

36. Alexander JJ. Blood-brain barrier (BBB) and the complement landscape. *Mol Immunol* 2018, 102, 26–31.

37. Girardi G, Lingo JJ, Fleming SD, Regal JF. Essential role of complement in pregnancy: from implantation to parturition and beyond. *Front Immunol* 2020, 11, 1681.

38. Walcheck B, Wu J. iNK-CD64/16A cells: a promising approach for ADCC?. *Expert Opin Biol Ther* 2019, 19, 1229–32.

39. Liu CC, Navratil JS, Sabatine JM, Ahearn JM. Apoptosis, complement and systemic lupus erythematosus: a mechanistic view. *Curr Dir Autoimmun* 2004, 7, 49–86.

40. Aharoni R, Eilam R, Arnon R. Astrocytes in multiple sclerosis-essential constituents with diverse multifaceted functions. *Int J Mol Sci* 2021, 22, 5904.

41. Abe N, Nishihara T, Yorozuya T, Tanaka J. Microglia and macrophages in the pathological central and peripheral nervous systems. *Cells* 2020, 9, 2132.

42. Liddelow SA, Barres BA. Reactive astrocytes: production, function, and therapeutic potential. *Immunity* 2017, 46, 957–67.

43. Leshchyns'ka I, Sytnyk V. Synaptic cell adhesion molecules in Alzheimer's disease. *Neural Plast* 2016, 2016, 6427537.

44. Rentzos M, Michalopoulou M, Nikolaou C, Cambouri C, Rombos A, Dimitrakopoulos A, et al. The role of soluble intercellular adhesion molecules in neurodegenerative disorders. *J Neurol Sci* 2005, 228, 129–35.

45. Chiarini A, Armato U, Hu P, Dal Pra I. CaSR antagonist (Calcilytic) NPS 2143 hinders the release of neuroinflammatory IL-6, soluble ICAM-1, RANTES, and MCP-2 from Abeta-exposed human cortical astrocytes. *Cells* 2020, 9, 1386.

46. Wang N, Sun Y, Yang H, Xu Y, Cai Y, Liu T, et al. Hashimoto's thyroiditis induces hippocampus-dependent cognitive alterations by impairing astrocytes in euthyroid mice. *Thyroid* 2021, 31, 482–93.

47. Fujii A, Yoneda M, Ito T, Yamamura O, Satomi S, Higa H, et al. Autoantibodies against the amino terminal of alpha-enolase are a useful diagnostic marker of Hashimoto's encephalopathy. *J Neuroimmunol* 2005, 162, 130–6.